RESEARCH ARTICLE

Proteome approaches combined with Fourier transform infrared spectroscopy revealed a distinctive biofilm physiology in *Bordetella pertussis*

Diego Omar Serra[1], Genia Lücking[2], Florian Weiland[3], Stefan Schulz[4], Angelika Görg[3], Osvaldo Miguel Yantorno[1] and Monika Ehling-Schulz[2, 5]

[1] Centro de Investigación y Desarrollo en Fermentaciones Industriales (CINDEFI, CONICET), Facultad de Ciencias Exactas, Universidad Nacional de La Plata, La Plata, Argentina
[2] Microbial Ecology Group, Department of Biosciences, WZW, Technische Universität München, Freising, Germany
[3] Fachgebiet für Proteomik, Technische Universität München, Freising, Germany
[4] Stefan Schulz Datensysteme, München, Germany
[5] Department for Farm Animals and Veterinary Public Health, University of Veterinary Medicine Vienna, Vienna, Austria

Proteome analysis was combined with whole-cell metabolic fingerprinting to gain insight into the physiology of mature biofilm in *Bordetella pertussis*, the agent responsible for whooping cough. Recent reports indicate that *B. pertussis* adopts a sessile biofilm as a strategy to persistently colonize the human host. However, since research in the past mainly focused on the planktonic lifestyle of *B. pertussis*, knowledge on biofilm formation of this important human pathogen is still limited. Comparative studies were carried out by combining 2-DE and Fourier transform infrared (FT-IR) spectroscopy with multivariate statistical methods. These complementary approaches demonstrated that biofilm development has a distinctive impact on *B. pertussis* physiology. Results from MALDI-TOF/MS identification of proteins together with results from FT-IR spectroscopy revealed the biosynthesis of a putative acidic-type polysaccharide polymer as the most distinctive trait of *B. pertussis* life in a biofilm. Additionally, expression of proteins known to be involved in cellular regulatory circuits, cell attachment and virulence was altered in sessile cells, which strongly suggests a significant impact of biofilm development on *B. pertussis* pathogenesis. In summary, our work showed that the combination of proteomics and FT-IR spectroscopy with multivariate statistical analysis provides a powerful tool to gain further insight into bacterial lifestyles.

Received: March 11, 2008
Revised: July 21, 2008
Accepted: July 22, 2008

Keyword:
Biofilm / *Bordetella pertussis* / FT-IR spectroscopy

1 Introduction

Bordetella pertussis is the etiologic agent of whooping cough, a human infectious disease of the upper respiratory tract. Although historically the occurrence of pertussis was associated with an acute infection, primarily in not- or under-immunized infants, a shift in the incidence of the disease towards adolescents and adults with the appearance of persistent asymptomatic or mild infections is becoming increasingly evident [1]. Recent reports support the hypothesis that *B. pertussis* could adopt a biofilm lifestyle as a strategy to colonize the host, but the mechanisms leading to persistent *B. pertussis* infections are largely unknown [2–4]. Biofilm is a community-based mode of existence of microbes in which cells are enclosed in a self-producing matrix and adhered to an inert or living surface [5]. In fact, many pathogens living in biofilms exhibit phenotypic traits that might be advantageous for their virulence, such as increased resistance to environ-

Correspondence: Dr. Monika Ehling-Schulz, Microbial Ecology Group, Department of Biosciences, WZW, Technische Universität München, Weihenstephaner Berg 3, D-85354 Freising, Germany
E-mail: monika.ehling-schulz@wzw.tum.de
Fax: +49-8161-714492

Abbreviations: FT-IR, Fourier transform infrared; **HCA,** hierarchical cluster analysis

mental stresses, host defences and conventional antibiotic therapy. Biofilms are therefore thought to be a major cause of persistent and chronic bacterial infections (for review see [5, 6]) and it is hypothesized that adults carrying *B. pertussis* biofilms may serve as important sources of infection by periodically shedding active cells, which could increase the pertussis incidence in infants [7].

The notable stress resistance of biofilms has been associated with physiological changes that microorganisms undergo during their transition from a planktonic life to a sessile existence (for review see [8, 9]). The assumption that these changes occur primarily as a consequence of adaptation to stressful and fluctuating physicochemical conditions encountered in the heterogeneous biofilm architecture, has led to the speculation that sessile cells resemble planktonic cells in stationary phase [10, 11]. However, this hypothesis of biofilm physiology is currently under discussion, raising the question whether changes taking place in sessile cells respond to the expression of biofilm-specific gene networks or physiological pathways [12].

The availability of the genome sequences for a number of bacterial pathogens has provided a framework for the development of functional proteomics in order to gain insights into host–pathogens interactions [13, 14]. The combination of proteomic tools with multivariate statistical methods paves the way for analysing complex arrays of datasets to get a more holistic picture of the relationship among samples [15]. Recent studies in *Pseudomonas aeruginosa* and *Bacillus cereus* demonstrated the power of multivariate proteomic approaches to investigate the distinctiveness of biofilm formation [16, 17]. Despite the great contribution of these approaches, a proper combination of proteomic data with metabolic and physiological data could significantly contribute to the understanding of the biofilm lifestyle of bacteria. Fourier transform infrared (FT-IR) spectroscopy, which provides global information about the whole cell macromolecules (lipids, carbohydrates, proteins and DNA/RNA) [18, 19], might present a valuable tool to complement proteomic data on a metabolic level in order to get an integral overview of sessile cell physiology.

In *B. pertussis* physiologic and pathogenic aspects have been extensively studied focusing on the planktonic mode of growth, while only a few works so far have considered the biofilm lifestyle of this bacterial pathogen [2, 20–22]. Therefore, generally only limited data is available on the nature of *B. pertussis* biofilm and information on a proteomic level is completely missing.

The aim of this work was to combine proteome studies with whole cell metabolic fingerprinting by FT-IR and multivariate statistical analysis to provide a first biofilm proteome profile for *B. pertussis* and gain a deeper insight into the biofilm physiology. The presented results show that biofilm formation in *B. pertussis* is a rather complex but distinct process.

2 Materials and methods

2.1 Bacterial strains and growth conditions

B. pertussis Tohama I strain (8132, Institute Pasteur Collection, Paris, France) was used throughout the study. Stock cultures were grown on Bordet–Gengou agar (BGA; Difco Laboratories, Detroit, USA) plates supplemented with 1% w/v Bactopeptone (Difco) and 15% v/v defribrinated sheep blood (Oxoid, Wesel, Germany) at 37°C for 72 h, and were subcultured for 48 h. For planktonic cultures, bacterial colonies grown for 48 h on BGA plates were inoculated into 500-mL Erlenmeyer flasks containing 100 mL of Stainer-Scholte (SS) broth and incubated at 37°C on a rotary shaker (160 rpm). Growth kinetics of suspended cells were monitored by periodically measuring the OD at 650 nm (OD_{650}) and plating out appropriate decimal dilutions of the cell suspensions. Cultures were harvested by centrifugation (15°C, $8000 \times g$, 20 min) at mid-exponential (24 h) and stationary (44 h) growth phases. Planktonic cells were washed with PBS or water for FT-IR spectroscopy experiments to remove any remaining components of the broth. Biofilms were grown on flat polypropylene beads (300 g; $\phi = 4.2$ mm, $h = 1.5$ mm, with an average density of 0.901 g/cm^3, Petroken, Argentina) in glass column reactors ($\phi = 6$ cm, $h = 45$ cm, IVA SA, Argentina). Experiments were carried out essentially as described previously by Bosch *et al* [21]. Briefly, a planktonic culture of *B. pertussis* (200 mL, $OD_{650} = 1.0$) grown in SS broth was used as inoculum for each column and incubated for 5 h at 37°C to allow cell attachment to the beads. Then, the suspension was drained to remove unattached cells and 200 mL of fresh SS broth were added to each column. Bioreactors were incubated aerobically (0.1 L/min) at 37°C for different time periods. At 24 h intervals, the broth was replaced with a fresh one. A fixed number of beads were recovered from the columns at different time points (0, 24, 48, 72, 96 and 120 h) to monitor growth of sessile cells (by viable-cell counting and crystal violet staining). Structural features of biofilm formation were examined by light microscopy. For viable cell count determination, the adhered cells were gently washed and detached from beads by slight agitation in PBS buffer before cell suspensions were plated on BGA plates. The number of attached colony-forming units (CFU/cm^2) was calculated considering dilutions, surface area of the bead and number of beads. For proteomic and FT-IR spectroscopy analysis, sessile cells were harvested after 72 h, when the biofilm achieved its mature structure. Beads were washed three times with sterile PBS buffer to remove unattached cells. Sessile cells were gently disaggregated in PBS buffer (or water for FT-IR spectroscopy), pelleted by centrifugation ($8000 \times g$ for 20 min at 15°C), washed twice, and stored at −80°C.

2.2 FT-IR spectroscopy

For FT-IR spectroscopy analysis, spectra of *B. pertussis* cells were recorded on a Spectrum One FT-IR spectrometer (PerkinElmer, USA). The washed pellets of biofilm and planktonic (exponential and stationary phase) cells were suspended in sterile distilled water to an OD_{650} of approximately 10. Each bacterial suspension (100 μL) were transferred to a ZnSe optical plate and dried in vacuum (3–6 kPa) to obtain transparent films. Absorbance spectra of all samples were recorded between 4000 and 650/cm [23]. To avoid spectral water vapour interferences each spectrum was measured under a continuous purge of dried air, co-adding 128 scans at 6/cm resolution. Prior to the analysis, baseline offset correction and vector normalization in the full spectral range were performed. Qualitative and semiquantitative analysis of spectral data, which is based on identifying differentiable bands among cell spectra associated with any macromolecular cell component, were carried out using the OPUS 3.0 data collection software.

2.3 Preparation of protein fractions

The method described by Ehling-Schulz *et al.* [24] was used with slight modifications. All cell samples were passed four times through a precooled French pressure cell (SLM AMINCO) at 140 mPa. Cell debris and membranes were harvested by ultracentrifugation (Beckman, USA) at $100\,000 \times g$ for 1 h at 15°C. The supernatants containing the soluble cytosolic proteins ('cytosol protein fraction'), were stored in a detergent buffer containing 7 M urea, 2 M thiourea, 1% DTT, 4% CHAPS and 2% Pharmalyte 3–10 at −80°C until use. The $100\,000 \times g$ pellets were washed two times (100 mM Tris–HCl pH 7.8), resuspended in the detergent buffer, sonicated, and extracted as described by Turlin *et al.* [25]. Supernatants containing the solubilized membrane bound and membrane-associated proteins ('membrane protein fraction') were collected by ultracentrifugation ($100\,000 \times g$ for 1 h at 15°C) and stored in aliquots at −80°C until analysis. The Total protein concentration was determined by using the 2-D Quant kit (GE Healthcare, Amersham Biosciences).

2.4 High-resolution 2-DE

Protein fractions were analysed by 2-DE according to Görg *et al.* [26, 27]. Aliquots of cytosolic protein fractions (150 μg) were separated in the first dimension using 18 cm long Immobiline DryStrips (GE Healthcare, Amersham Biosciences) with a pH gradient of 4–7 or 6–9. Protein samples were focused using an Ettan IPGphor 3 IEF unit (GE Healthcare, Amersham Biosciences) under the following conditions: step 1, 150 V ramped to 600 V over 3 h; step 2, 600 V ramped to 8000 V over 1 h, and step 3, 8000 V for a total of 42.0 kVh (pH 4–7) or 49.0 kVh (pH 6–9). IEF of proteins from the membrane fraction was carried out similarly on Immobiline DryStrips of pH 4–7 for a total of 45.0 kVh. Before the second dimension, strips were equilibrated for 2×15 min in equilibration buffer (6 M urea, 2% SDS, 30% glycerol, 0.05 M Tris–HCl pH 8.8) containing 1% DTT and 4% iodoacetamide, respectively. SDS-PAGE was carried out vertically in an Ettan DALT II system (Amersham Biosciences) using 12.5% polyacrylamide gels. Resolved proteins were routinely stained with silver nitrate or alternatively with colloidal Coomasie blue (Roti-Blue, Roth, Karlsruhe, Germany) for protein identification purposes. All experiments were performed in triplicate. Reproducibility of the 2-DE was tested by running the same samples at least three times on independent gels. A total of about 120 gels have been run during this approach.

2.5 Image analysis and data processing

Silver stained gels were scanned using a calibrated flatbed scanner (HP Scanjet 4890, Hewlett-Packard, Germany) and gel analysis was performed with the Proteomweaver imaging software Version 4.0 (BioRad Laboratories, Munich, Germany). Replicates from three independent growth experiments were included in computer assisted image analysis and reproducibility of the growth experiments was tested by principal component analysis (PCA) (see Section 2.7). In a first step, individual gels were prematch normalized using the standard Proteomweaver algorithm, spots were detected automatically and gels were pair matched. Then, all gels were matched to each other, creating a group of 'superspots'. At this step, mismatches were carefully checked and edited manually. Spot intensities were normalized using the pair match-based normalization algorithm of the Proteomweaver software. Differences in spots intensities values between the tested samples as well as the presence or absence of spots in a specific condition were evaluated using the following criteria: statistical significance ≤ 0.05 (*t*-test) and differential tolerance, fold change ≥ 3. Proteins present in detectable amounts or absent in only one of the tested growth conditions were analysed by the group frequency, which represent the total number of gel images corresponding to a particular condition in which the specific spot was detected. Generated and normalized data were exported to Microsoft EXCEL for further statistical analysis.

2.6 In-gel trypsin digestion and MALDI-TOF MS

Selected protein spots were analysed by MALDI-TOF MS. In brief, spots were cut from CBB stained gels, destained with 25 mM ammonium bicarbonate and 50% ACN and dried before addition of modified trypsin (Promega); 10 μL of 12.5 ng/μL in 50 mM ammonium bicarbonate. After incubation at 37°C for 12–20 h, the products were recovered by sequential extractions with 50% ACN and 0.5% TFA. Extracts were lyophilized and resuspended in 3 μL of 50% ACN and 0.5% TFA for analysis by MALDI-TOF MS. Peptide mass fingerprints were obtained by using a solu-

tion of 2 mg/mL CHCA, 1% TFA, 50% ACN and 10 mM ammonium monobasic phosphate as matrix. MS was performed by using the Ettan Z^2 MALDI-TOF MS (Amersham Biosciences) with a UV nitrogen laser (337 nm) and harmonic reflectron; mode: positive-ion reflectron mode at 20 KV with delayed extraction mode and low mass rejection; calibration: peptide samples (Angiotensin II, ACTH 1-39) and internal standard (trypsin autodigestion fragments). Proteins were identified by searching the monoisotopic masses against the database of *B. pertussis* Tohama I curated by NCBI (accession: NC 002929; protein coding: 3436; www.ncbi.nlm.nih.gov) with the implemented software Ettan MALDI-TOF Pro Evaluation Module V2.0 (Amersham Biosciences). One missed cleavage *per* peptide was allowed, and a mass tolerance of 10 ppm was used in all searches. Partial modifications of proteins by carbamidomethylation of cysteines and oxidization of methionines were taken into account. Proteins were considered as identified if at least five peptides were matched and the expectation value was smaller than 0.05.

2.7 Multivariate statistical analysis

For multivariate analysis of the FT-IR spectral datasets corresponding to the different bacterial populations, including also the *in silico* spectra, spectral regions 3000–2800 and 1800–750/cm were considered. These regions include the IR absorption bands of the main cell macromolecules. Hierarchical cluster analysis (HCA)-based on PCA [28] was carried out using the 'identity' and 'cluster analysis' modules of the OPUS 3.0 software [23]. In parallel, PCA and HCA were also used to interpret the variations in the protein profiles revealed by 2-DE analysis. Statistical analysis of proteome data was essentially performed as described by Ehling-Schulz *et al.* [24]. Protein spot data were normalized and standardized as described previously, exported from the Access database generated by the Proteomweaver software and imported into Microsoft EXCEL. Statistical analysis was carried out using the software package XLSTAT 2007 (Addinsoft™, New York, USA). Datasets from two complete, independent growth experiments were included in the analysis.

The *in silico* spectra were obtained by using the OPUS 3.0 data collection software package (Bruker, Germany). These spectra corresponded to hypothetical spectra representing virtual mixtures of planktonic populations (25:75, 50:50 and 75:25% of exponential and stationary populations, respectively). For example, a hypothetical spectrum of a cell mixture composed of 25% of a population A and 75% of a population B results from the following arithmetic operation applied to the FT-IR spectra: $0.25 \times$ spectrum condition A + $0.75 \times$ spectrum condition B. A similar approach was carried out to generate *in silico* mixed proteomes according to Vilain and Brözel [17]. *In silico* mixed spectra and proteomes were statistically analysed as described above.

2.8 Alcian blue staining and light microscopy examination

Biofilms developed on transparent flat polypropylene beads and cells harvested from planktonic cultures were gently washed in PBS. After the washing steps, they were stained with 0.1% aqueous alcian blue (Sigma, St. Louis, Mo.) and gently washed $3 \times$ with PBS. The dye alcian blue specifically stains acidic polysaccharides. It reacts with the acidic functional groups of polysaccharides yielding an insoluble nonionic precipitant. Light microscopy was conducted at a magnification of 1000-fold under oil immersion using a Leica DMLB microscope (Leica Microsystems, Wetzlar, Germany) equipped with a cooled CCD digital camera.

3 Results

3.1 Analysis of subcellular protein fractions

B. pertussis cells were grown in parallel as free-swimming planktonic cultures (free-floating cells in suspension; Fig. S1 of Supporting Information) and as biofilms on a polypropylene surface to comparatively assess the impact of biofilm growth in a mature stage on the *B. pertussis* proteome. Light microscopy, which allows monitoring of spatial changes occurring in a biofilm, showed that the stage of maximal biomass formation ('exponential-like stage') coincides with the development of a mature biofilm structure characterized by irregularly shaped cell clusters scattered on the surface (see Fig. S2 of Supporting Infomation). Biofilm cultures were sampled when this mature structure was achieved, whereas planktonic cultures were sampled at exponential and stationary growth phase (Fig. 1). Total protein was isolated and sub-fractionated prior to electrophoresis to gain a better understanding of the localization of proteins influenced by the mode of growth. Representative images of *B. pertussis* subproteomes obtained from cells grown in either planktonic or in biofilm mode are presented in Fig. 2. In the cytosolic protein fraction a total of about 1000 protein spots (pH 4–9), and in the membrane fraction a total of about 300 protein spots (pH 4–7) could be detected reproducibly in the range of 10 to 110 kDa. Differential 2-DE analysis revealed 8% of the spots of the cytosol and 10% of the membrane subproteomes analysed to be specifically regulated in *B. pertussis* biofilm cells. Within the group of proteins specifically regulated in biofilm, those upregulated or expressed *de novo* (78 proteins) were predominant while only a few proteins (22 proteins) showed significant down regulation or were absent (data not shown).

3.2 Metabolic fingerprinting by FT-IR spectroscopy

FT-IR spectroscopy has been successfully applied to characterize the structural and biochemical composition of a wide range of biological samples, including microbial cells

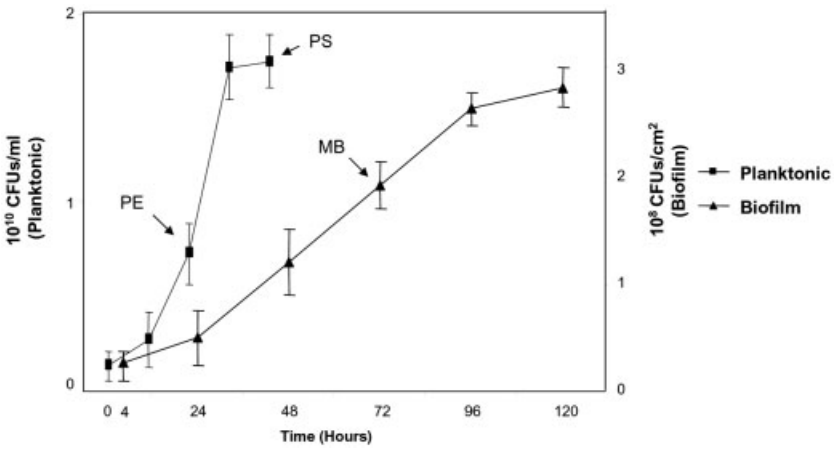

Figure 1. Growth kinetics of planktonic and biofilm *B. pertussis* Tohama I cells in Stainer–Scholte medium at 37°C. Planktonic cells (■) were harvested from Erlenmeyer flasks, whereas sessile cells (▲) were recovered from flat polypropylene beads of a glass column bioreactor. Arrows indicate the harvesting point for FT-IR spectroscopy and proteomic analysis. Results are averages of at least three independent experiments. PE: planktonic cells in exponential phase; PS: planktonic cells in stationary phase and MB: cells in mature biofilm.

[18, 29–32]. It allows the analysis of the molecular composition of a sample using the interaction between the infrared (IR) radiation and the sample. As a result of this interaction, the sample transmits and reflects the IR radiation, which is translated into an IR absorption spectrum [23].

In this study, a qualitative and semiquantitative FT-IR spectroscopic analysis was performed to decipher physiological features which are particularly associated to the *B. pertussis* biofilm lifestyle in a mature state. Therefore, *B. pertussis* cells were grown in parallel as planktonic cultures and as biofilms. Cells were harvested at the time points indicated in Fig. 1, washed, dried on ZnSe optical plates and spectra were recorded on a Spectrum One FT-IR spectrometer. Evaluation of IR spectral data was performed using the OPUS software (for details see Section 2). Comparative analysis of spectral data (Fig. 3) revealed a significant increase in the intensity of absorption bands assigned to carbohydrate functional groups (spectral region: 1200–900/cm) in sessile cells. In addition, bands assigned to vibrational modes of carboxylate (spectral bands: 1400–1410 and 1375/cm) and ester groups (spectral band: 1260/cm) were also found to be distinctively increased in biofilm grown cells (Fig. 3).

3.3 Differentiation of biofilm and planktonic *B. pertussis* populations by proteomic and FT-IR spectroscopy multivariate statistical analysis

2-DE coupled with PCA, a nonparametric multivariate analysis, was used to investigate on protein level the distinctiveness of *B. pertussis* biofilm cells (MB) with respect to those grown planktonically in exponential (PE) and stationary phase (PS). PCA of two independent datasets, which included all spots detected in the cytosolic (pH 4–7 and 6–9) and membrane-associated (pH 4–7) protein fractions, extracted three components (PCs) with eigenvalues greater than 1. Statistically, the differences found in the gel profiles are explained by the first three factors, collectively accounting for 84 and 98% of the variability in the cytosolic and membrane datasets, respectively. The first factor was the same for all protein samples analysed and accounted for 56% (cytosolic) and 48% (membrane) of the variance. The second and third components (PC2 and PC3) accounted together for about 30% (cytosolic) and about 50% (membrane) of the 2-D gel profiles' variance. The inter-variable angles between vectors representing the three populations in the biplots show no significant correlation between them, indicating clear differences between biofilm and planktonic conditions and between both planktonic conditions (Fig. 4). Additionally to PCA, a multivariate HCA of subproteome datasets (pH 4–7) was performed. In this analysis hypothetical subproteomes created to simulate the subproteomes of virtual mixtures of both planktonic populations (25:75, 50:50 and 75:25% of exponential and stationary populations respectively) were included to test whether the biofilm grown cells (MB) are merely composed of a mixture of exponential (PE) and stationary (PS) planktonic grown cells. HCA of experimentally and *in silico* generated protein profiles clearly separated biofilm grown cells from planktonic grown cells (see Fig. 5A and Fig. S3 of Supporting Information). The stationary condition had a greater influence on the subproteome profiles of the hypothetical mixtures than the exponential one (Fig. 5A).

In parallel to the multivariate proteomic approaches, information acquired by FT-IR spectroscopy, including some virtual mixtures of spectral datasets (for details see Section 2), was analysed by HCA based on PCA. The first three components derived from PCA (which comprised 90% of the variance of the dataset considering the IR absorption bands in the spectral regions 3000–2800 and 1800–750/cm) were used for HCA analysis. HCA produced two major groups of spectral patterns that strongly separated between biofilm and planktonic populations (Fig. 5B). The latter group is represented by independent spectra of exponential and stationary phase populations and by *in silico* spectra of virtual mixtures of these two planktonic populations (ratio: 25:75, 50:50 and 75:25%). In summary, multivariate FT-IR spectroscopy analysis discriminated within this planktonic group separating spectra in groups corresponding to exponential and sta-

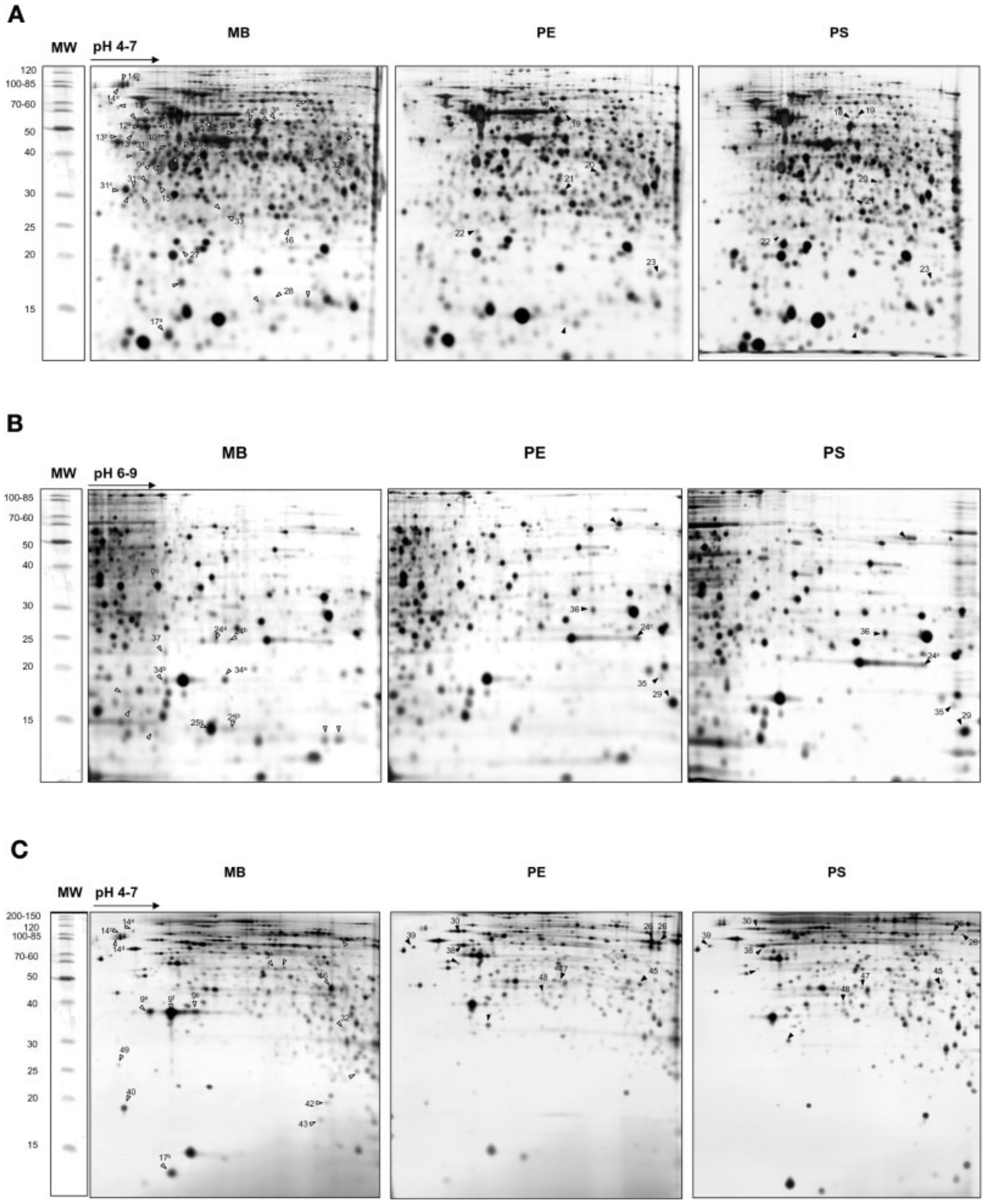

Figure 2. Representative images of *B. pertussis* cytosolic (A, B) and membrane (C) protein profiles. Proteins at least three-fold over-expressed or expressed *de novo* in biofilm cells are indicated by open arrows in gels corresponding to the biofilm (MB). Proteins at least three-fold downregulated or completely repressed in biofilm are shown by solid arrows in gels corresponding to both planktonic conditions (PE and PS). Numbers refer to identify proteins listed in Table 1. Abbreviations as in Fig. 1.

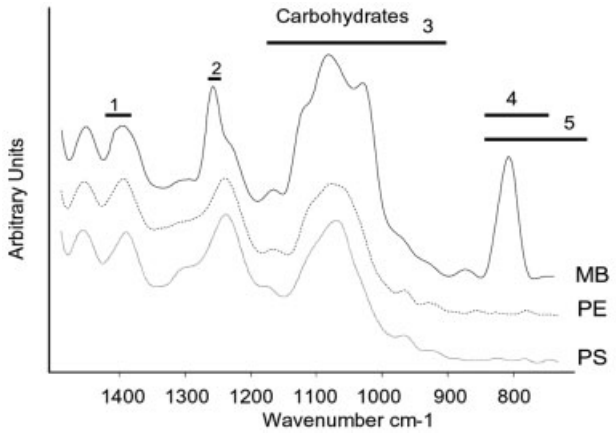

Ref. in Fig	Assignement to main spectral bands	Ref. in bibliography
1	-C=O symmetric stretching and C-O bending of COO^-	21, 23, 30
2	-C-O-C ester asymmetric stretching	21, 23, 30
3	-C-OH, C-O-C and C-O ring vibrations of carbohydrates	23, 31, 32
4	glycosidic linkage type "anomeric region"	29, 31
5	"fingerprint region"	23

Figure 3. Spectral region (1500–700/cm) of infrared spectra corresponding to *B. pertussis* cells harvested from biofilm and planktonic cells. Each spectrum represents average of spectra corresponding to three independent experiments. Spectra were full range vector normalized. Numbers in the figure correspond to IR absorption band of functional group described in the inserted table. Abbreviations as in Fig. 1.

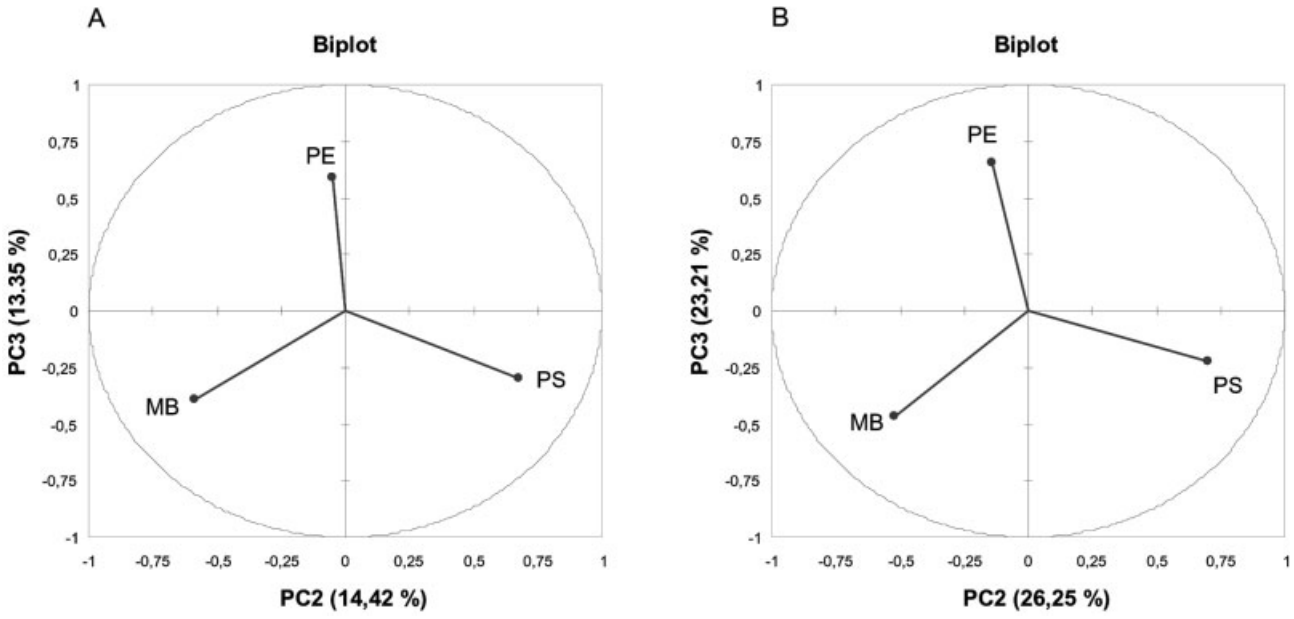

Figure 4. Biplots displaying the second and third components derived from PCA of cytosolic (A) and membrane (B) subproteomes. Percentages between brackets indicate the variability in dataset associated with each component. Abbreviations as in Fig. 1.

tionary phase cells. In addition, virtual mixtures of spectral data were clearly discriminated from those of the pure planktonic populations, more closely resembling stationary cells than exponential cells (Fig. 5B).

3.4 Identification of proteins differentially regulated in biofilm lifestyle of *B. pertussis* by MALDI-TOF MS

Differentially expressed proteins in sessile cells were excised from gels and subjected to MALDI-TOF MS PMF analysis (Table 1). Proteins identified by MALDI-TOF MS are depicted in Fig. 2. As expected, some proteins were present in multiple forms (*e.g.* 24a, 24b and 24c depicted in Fig. 2B), probably representing isoforms due to PTMs. The group of cytosolic proteins identified by PMF analysis encompassed mainly proteins involved in central and intermediary metabolism/biosynthesis, adaptation and stress, as well as cellular processes and regulatory events; the group of membrane proteins was mainly represented by proteins involved in adhesion, transport and binding activities (Table 1).

The most noteworthy findings were proteins overexpressed or expressed *de novo* in the mature biofilm, which are involved in polysaccharide biosynthesis pathways (Fig. 6).

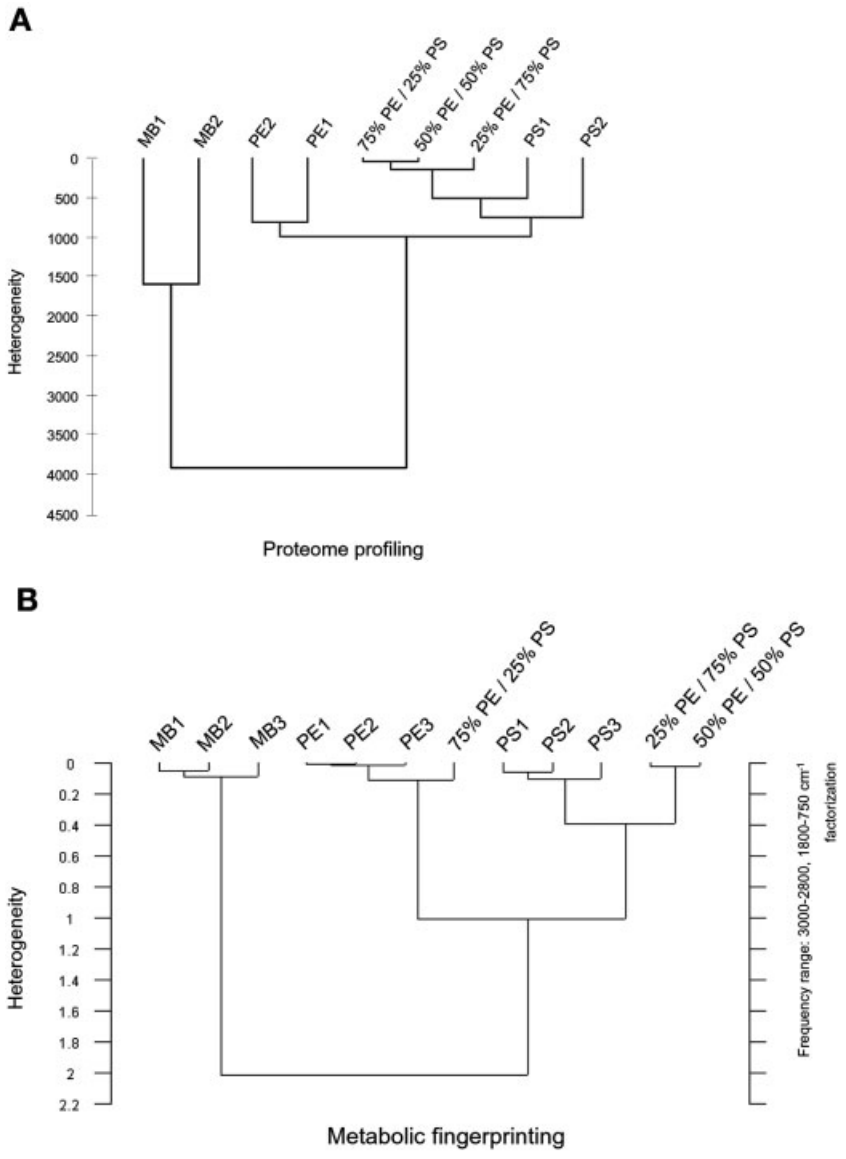

Figure 5. (A) Dendrogram resulting from HCA of proteome profiles from biofilm and planktonic cells. The dendrogram includes *in silico* proteome profiles created to simulate virtual mixtures of the two planktonic populations (75:25, 50:50 and 25:75% of PE and PS, respectively). (B) Dendrogram resulting from an HCA based on PCA using the first three components (which capture 90% of the variance in the dataset) between 3000–2800/cm and 1800–750/cm. The dendrogram displays spectra of three independent experiments corresponding to the different growth conditions and also includes *in silico* spectra created to simulate virtual mixtures of the two planktonic populations (75:25, 50:50 and 25:75% of PE and PS, respectively). Abbreviations as in Fig. 1. The numbers indicate independent growth experiments: PE1, PS1, MB1 refer to the first experiment, PE2, PS2, MB2 to a second experiment, and PE3, PS3, MB3 to samples obtained from a third experiment.

One of these proteins, which showed a three-fold higher expression in biofilms, is annotated as a polysaccharide biosynthesis protein, also referred as WbpO (UDP-*N*-acetyl-D-galactosamine dehydrogenase). Another protein found more than four-fold upregulated in biofilms corresponds to a phosphoglucomutase enzyme named Pgm, which is predicted to exhibit both phosphoglucomutase and phosphomannomutase activity. Finally, a third protein, only detected in the biofilm condition (Figs. 2A and 6) and annotated as thymidine diphosphoglucose 4,6-dehydratase (BP0665), is a nucleoside epimerase/dehydratase involved in carbohydrate metabolism. Other proteins that were grouped in the central and intermediary metabolism/biosynthesis category include proteins involved in amino acid and purine metabolism, which were mainly found to be over-expressed in biofilms (see Table 1 and Fig. 2).

Another remarkable finding linked to the *B. pertussis* biofilm lifestyle is the over-expression of the S-adenosylmethionine synthetase enzyme in biofilms, which could be involved in a putative quorum sensing regulatory circuit. In addition, expression of proteins known to be associated with bacterial virulence, such as the BvgA transcriptional activator, the pertactin autotransporter and putative adhesins such as BipA and the prominent outer membrane porin protein (BP0840), was altered in biofilms.

3.5 Alcian blue staining of biofilm and planktonic cells

The dye alcian blue specifically stains acidic polysaccharides. It was therefore used to assess the production of an acidic-type polysaccharide in *B. pertussis* cells grown either in bio-

Table 1. Differentially expressed proteins in *B. pertussis* biofilms grown on polypropylene beads identified by MALDI-TOF/MS

Functional category	Protein name; putative function	Accession no.	Spot no.[a)]	Expression[b)]	Mass (KDA)	p*I*	Expectation/ % coverage	Matching peptides
Central and intermediary metabolism/ biosynthesis	Adenylosuccinate synthetase; role in the *de novo* pathway of purine nucleotide biosynthesis; involvement in alanine and aspartate metabolism	Q7VWM1	1	+	46.76	6.7	0.003/30.1	10
	Amidophosphoribosyltransferase; involvement in the purine and glutamate metabolism	Q7VYD4	18	Off	55.56	5.7	0.003/22.7	9
	N-acetyl-γ-glutamyl-phosphate reductase; it is similar to many proteins involved in arginine biosynthesis	Q7VUW0	44	(+)	37.8	6.6	0/35.3	9
	Serine hydroxymethyltransferase; role in the interconversion of serine and glycine	Q7VUW7	45	−	44.8	6.5	0.002/34.5	12
	GMP synthase (glutamine-hydrolysing); involvement in the purine and glutamate metabolism	Q7VVM4	4a,b	+	57.85	5.6	0/40	8-15
	Glutamate dehydrogenase; involvement in glutamate, arginine, proline, D-glutamine and D-glutamate metabolism	Q7VXC5	46	+	46.3	6.3	0/31	11
	S-adenosylmethionine synthetase; involvement in the methionine and seleno amino acid metabolism; *S*-adenosylmethionine is a precursor and intermediary in the biosynthesis of acyl-homoserine lactone and AI-2 autoinducer signals; putative involvement in quorum sensing signalling	Q7VUL5	10	+	41.98	5.1	0/23.5	8
	Diaminopimelate decarboxylase; role in the lysine biosynthetic process *via* diaminopimelate	Q7VT97	47	−	46.4	5.7	0.002/37.1	11
	Acetolactate synthase small subunit; acetolactate synthases are a group of biosynthetic enzymes that are capable of *de novo* synthesis of the branched-chain amino acids	Q7VZU5	43	+	18.1	6.3	0.001/28.5	7
	Putative AMP-binding protein; probable involvement in glycolisis/gluconeogenesis, pyruvate and propanoate metabolism and reductive carboxylate cycle	Q7VW88	19	−	62.27	5.8	0.012/28.6	11
	Phosphoenolpyruvate synthase; role in pyruvate metabolism and involvement in reductive carboxylate cycle	Q7VYB3	30	−	86.22	4.8	0.001/28.1	9
	Succinyl-CoA synthetase, β chain; involvement in citrate cycle, pyrutave and propanoate metabolism and reductive carboxylate cycle	Q7VVU5	8	+	40.92	5.2	0.001/31.5	8
	Inorganic pyrophosphatase; involvement in oxidative phosphorylation	Q7VVV3	27	On	20.02	5.3	0.009/38.8	6
	ATP synthase subunit α; involvement in oxidative phosphorylation	Q7VU46	3a,b	+	55.46	5.6	0.009/15	12
	ATP synthase subunit β; involvement in oxidative phosphorylation	Q7VU44	12a,b	+	50.51	4.9	0.001/30.7	12-15
	CDP-6-deoxy-δ-3,4-glucoseen reductase; probable involvement in electron carrier and iron–sulphur binding activities	Q7VXF7	48	−	38.0	5.6	0/25.1	8
	Putative hydrolase; it displays α/β hydrolase activities	Q7VUJ2	21	−	32.86	5.6	0/27.6	10
	Putative transferase; it displays phosphoribosyl transferase activities	Q7VWM2	42	+	20.4	6.3	0/30.1	8
	Putative acetyltransferase; role in acetyl group transfer from acetyl coenzyme A to a primary amine in a wide variety of acceptor molecules; involvement in diverse cellular functions	Q7VTK7	28	On	16.08	5.6	0/56.5	8
	Polysaccharide biosynthesis protein; belongs to UDP-glucose/GDP mannose dehydrogenase family; Similar to *S. typhi* Vi polysaccharide biosynthesis protein VipA or TviB and to *P. aeruginosa* Wbp0	Q7VUE7	5	+	46.71	5.5	0/27.1	12

Table 1. Continued

Functional category	Protein name; putative function	Accession no.	Spot no.[a)]	Expression[b)]	Mass (KDA)	p*I*	Expectation/ % coverage	Matching peptides
	Phosphoglucomutase; protein predicted to display both phosphoglucomutase and phosphomannomutase activities; similar to *P. aeruginosa* phosphomannomutase AlgC and to *Neisseria meningitidis* phosphoglucomutase Pgm	Q7VUF5	41	+	49.0	5.2	0/30.5	10
	Thymidine diphosphoglucose 4,6-dehydratase; it is a nucleoside-diphosphate-sugar epimerase/dehydratase. Probably involvement in cell envelope biogenesis, outer membrane/carbohydrate transport and metabolism	Q7VRZ4	32	+	35.31	6.1	0.035/32.5	8
Adaptation and stress proteins	60 kDA Chaperonin; promotes refolding of misfolded polypeptides especially under stressful conditions	P48210	31a-e	On	57.46	5.1	0/28.5	8-11
	Chaperone protein hscA; involvement in the maturation of iron–sulphur cluster-containing proteins. Has a low intrinsic ATPase activity which is markedly stimulated by hscB	Q7VXG7	39	−	65.2	4.5	0/35.8	14
	Putative GrpE chaperone; participates actively in the response to hyperosmotic and heat shock by preventing the aggregation of stress-denatured proteins, in association with dnaK	Q7VVY0	40	+	19.6	4.5	0.005/30.3	8
	Curved DNA-binding protein; similar to *E. coli* curved DNA-binding protein CbpA; presents a DnaJ-domain, which is part of a chaperone (protein folding) system	Q7VZB0	15	+	34.73	5.6	0.011/21.3	7
	Trigger factor: *B. pertussis*; peptidyl-prolyl *cis*/*trans* isomerase; promotes folding of newly synthesized proteins	Q7VXI8	13a-c	On	47.6	5	0.001/32.6	8-9
	Universal stress family protein; involvement in response to stressful conditions	Q7VYK8	25a,b	+	15.12	8	0.015/58.2	6
	Antioxidant protein; involvement in redox regulation of the cell. May play a role in the regulation of phospholipid turnover as well as in protection against oxidative injury	Q7VZE7	33	On	23.76	5.6	0.008/46.5	8
	Molybdopterin biosynthesis protein; members of the MoeA family are involved in biosynthesis of the molybdenum cofactor (MoCF), an essential cofactor of a diverse group of redox enzymes	Q7VY89	6	+	45.39	5.3	0.032/32.8	9
	Chaperone protein htpG; heat shock protein; involvement in response to stressful conditions	Q7W0M8	38	−	71.14	5	0/23.6	8
Cellular process and regulatory proteins	Cell division protein FtsZ; GTPase; similar structure to tubulin; forms ring-shaped polymers at the site of cell division	Q7VUQ8	11	+	41.41	5	0.007/27.4	7
	50S Ribosomal protein L10; it binds the two ribosomal protein L7/L12 dimers and anchors them to the large ribosomal subunit	Q7W0S1	29	−	18.47	9.9	0.008/32.8	7
	BvgA transcriptional activator; cytoplasmic DNA binding protein that, when phosphorylated, activates the expression of a broad array of virulence factors	P0A4H2	24a-c	–	22.93	8.8	0/34.9	8-12
Adhesion, transport and binding Proteins	Pertactin; 68–70-kDa surface protein; mediates eukaryotic cell binding *in vitro*; enhances protective immunity	P14283	2	+	93.43[c)]	9.2	0/35.1	12
	Putative outer membrane ligand binding protein; similarity with intimin of enteropathogenic and enterohemorrhagic *E. coli* and invasion of *Yersinia spp.*; unknown role in *Bordetella* lifecycle	Q7VZ27	14a-e	On	137.18	6.3	0/20.3	15
	Outer membrane porin protein; high homology with PIA porin of *Neiseria gonorrhoeae* and the OmpC of *E. coli*; probable role in elicit protective immunity	Q04064	9a-g	+	41.03[c)]	5.5	0.005/23.6	7-9

Table 1. Continued

Functional category	Protein name; putative function	Accession no.	Spot no.[a)]	Expression[b)]	Mass (KDA)	p*I*	Expectation/ % coverage	Matching peptides
	Outer membrane protein A precursor; highly similar to the immunogenic outer membrane protein A precursor OmpA from *Bordetella avium*	Q7VZG6	34a,b	–	20.97[c)]	9.1	0.023/49.7	8
	Putative iron–sulphur binding protein; similar to *E. coli* Mrp protein; probable role in multiple resistance and pH adaptation	Q7VY87	7	On	38.18	5.4	0/35.9	11
	Putative periplasmic solute binding protein; similar to Rhizobium loti ABC transporter, periplasmic binding protein MLL8313; probable involvement in inorganic ion transport	Q7VUK6	20	Off	33.39	6	0.001/32.5	10
	Putative outer membrane protein; similarity with TonB-dependent receptor protein in *B. avium*. Similar to *Neisseria meningitidis* putative outer-membrane receptor protein NMA1161	Q7VUK9	26	Off	77.81	6.1	0/47	22
	Putative outer membrane protein; similar to *Vibrio cholerae* outer membrane protein OmpW; probable role in adaptive response to stress conditions	Q7VT02	37	+	23.01	9.2	0.028/27.4	8
	Putative membrane protein; similar to *Caulobacter crescentus* nodulin-related protein Cc0717; unknown function	Q7VYA1	16	On	22.76	8.2	0.015/15	7
	Putative membrane protein; protein containing LysM domain; unknown function	Q7VT64	17a,b	+	19.29	6.1	0.04/24.6	7
	Putative exported protein; similar to *Vibrio cholerae* hypothetical protein Vc1523 Unknown function	Q7VY76	36	–	29.02	9.3	0.03/25.4	6
Others	Hypothetical protein; uncharacterized conserved protein	Q7VTQ0	23	–	18.79	6.2	0.016/43.5	8
	Hypothetical protein; uncharacterized protein	Q7VUK7	22	–	20.82	4.9	0.008/39.9	8
	Hypothetical protein; uncharacterized conserved protein	Q7VUZ9	35	–	17.83	8.7	0.019/27.1	6
	Hypothetical protein; uncharacterized protein	Q7W0N5	49	+	29.1	5.1	0.008/30.1	8

The protein spots were identified by MALDI-TOF MS using PMF. Proteins specifically expressed in sessile cells according to the following criteria: $p \leq 0.05$ (*t*-test).

a) a–g refer to protein isoforms indicated in Fig. 2.

b) +, at least three-fold over-expressed; –, at least three-fold under-expressed; On, present only in biofilm; Off, absent in biofilm.

c) Molecular weight of the unprocessed precursor.

films or planktonically. Light microscopy showed an increased production of acidic polysaccharide in *B. pertussis* biofilm cells, which is in accordance with FT-IR spectroscopy data and protein identification. A considerable amount of alcian blue-stained material was associated with biofilm cells, whereas cells grown in planktonic cultures were only poorly stained (Fig. 7).

4 Discussion

This work investigated the distinctiveness of the physiological response taking place in the *B. pertussis* biofilm in contrast to planktonic growth. Previous studies have focused on comparing physiological features between biofilm and planktonic populations for different bacteria [9, 14, 33, 34]; however, none of these studies have addressed this question by combining proteomic and FT-IR spectroscopy techniques.

Independent multivariate analysis of 2-DE and FT-IR spectroscopy datasets discriminated *B. pertussis* biofilm cells (MB) from those grown planktonically (PE and PS), providing evidence that sessile cells display a distinctive physiology in the mature biofilm (Fig. 5). These results are consistent with those reported for *P. aeruginosa* and *B. cereus* [16, 17, 35] which, based on multivariate proteomic approaches (PCA), indicated that biofilm formation has a distinctive and specific impact on the bacterial physiology compared to planktonic growth. However, in the past the existence of a biofilm specific physiology has been questioned based on microarray data. Transcriptome analysis of *P. aeruginosa* cells grown either in a biofilm or planktonic mode revealed less than 1% difference in gene expression, leading to the assumption that biofilms simply represent a population of bacteria at different growth stages [36, 37]. On the other hand, data from proteome studies revealed differences between biofilm and planktonic growth in the range of 10–40% [38], which is in accordance with data presented in this work. Univariate

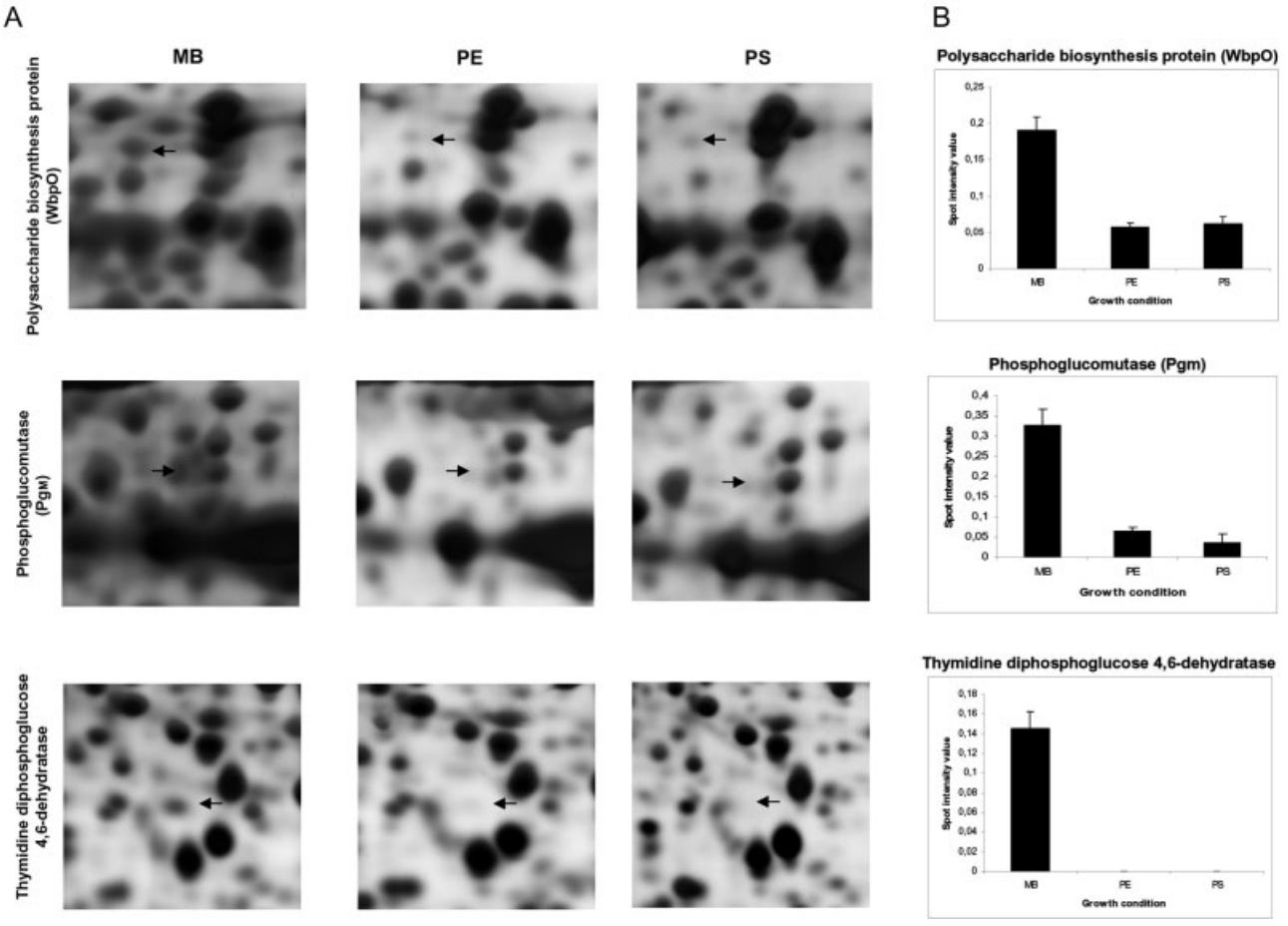

Figure 6. (A) Zoom gel images of protein spots associated with carbohydrate metabolism displaying different expression in biofilms (MB) compared to planktonic (PE and PS) conditions. (B) Graphics show average and SD of spot intensity values corresponding to three independent experiments for each growth condition. Abbreviations as in Fig. 1.

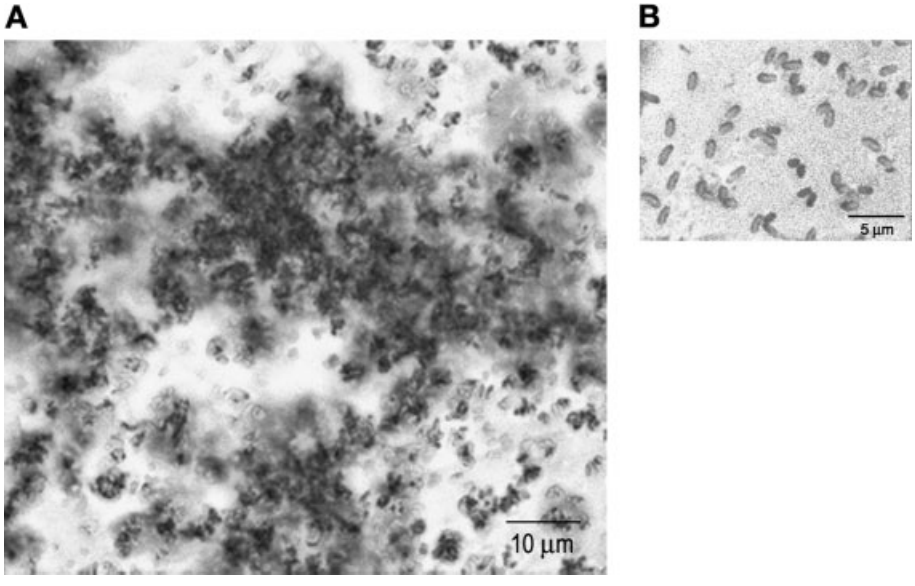

Figure 7. Light microscopy images of wild type Tohama I *B. pertussis* cells grown in biofilm on polypropylene surface over 72 h (A) and in planktonic cultures at exponential phase (B), stained with alcian blue (0.1% in water).

statistical analysis of proteome profiles from *B. pertussis* revealed about 8% (cytosolic subproteome) to 10% (membrane subproteome) of the proteins to be differentially regulated in biofilms (data not shown). Particularly, by including hypothetical 2-D gel and FT-IR spectroscopy datasets created to simulate mixtures of exponential and stationary planktonic populations in HCA, it was demonstrated that the biofilm phenotype is not the result of a mixture of planktonic populations at different stages (Fig. 5). The discrepancy observed between transcriptome and proteome data highlights the importance of investigations at post-transcriptional and post-translational, and probably even at metabolic levels.

Analysis of the *B. pertussis* biofilm proteome showed that the particular biofilm physiology correlates with a relative over-expression and *de novo* expression of proteins, demonstrating that sessile cells remain in an active growth state. The influence of biofilm formation seems to be more pronounced on the membrane than on the cytosol, since higher percentages of variance associated to PC2 and PC3 were found for the membrane subproteome (49.5%) than for the cytosolic one (27.8%). Identification of protein spots by MALDI-TOF MS showed that cytosolic proteins upregulated or expressed *de novo* in biofilm correspond to proteins mainly involved in central and intermediary metabolism/biosynthesis, adaptation and stress, as well as cellular and regulatory processes, while membrane-associated protein spots distinctively regulated in biofilms could be mainly linked to proteins involved in adhesion, transport and binding activities (Table 1). Coincidently with these results, sets of proteins belonging to the same functional categories were also found to be differentially regulated in biofilms of other microorganisms (for review see [38]), supporting the idea that certain physiological features particularly associated with biofilms could be common for different bacteria.

One of the most outstanding and distinctive physiological features of the *B. pertussis* biofilm lifestyle is linked to the carbohydrate metabolism. Quantitative and semi-quantitative FT-IR analysis demonstrated a relative increase in spectral bands assigned to carbohydrate functional groups for the sessile population, indicating an increase in carbohydrate production in the mature biofilm (Fig. 3). Increased IR signals for carboxilate and ester groups indicate the presence of an acidic-type polysaccharide with acetyl groups. In the same way, three proteins involved in polysaccharide biosynthesis pathways, found over-expressed and expressed *de novo* in biofilms, were identified. Two of these proteins correspond to an UDP-*N*-acetyl-D-galactosamine dehydrogenase (BP3150) and a phosphoglucomutase (BP3141), which are encoded together in a putative polysaccharide biosynthesis locus (BP3141-3157), not yet known to be involved in biofilm formation. The first enzyme (BP3150) shared 99.7% of identity with a protein from another genetic locus (BP1619-1631), previously described to be involved in polysaccharide production [39], while no homologue of the second enzyme (BP3141) was detected in the latter locus (data not shown). Both loci, BP3141-3157 and BP1619-1631, encode enzymes involved in polysaccharide biosynthesis, modification and transport (www.ncbi.gov.org), nevertheless they have quite different gene organization. The expression of the whole BP1619-1631 locus is still uncertain since its 3′-region contains insertion sequence element-mediated rearrangements [39], whereas the expression of two enzymes from the uncharacterized polysaccharide biosynthesis locus (BP3141-3157) was clearly demonstrated in this work. The genes from these loci are homologous to the *Salmonella typhi* Vi antigen biosynthesis enzymes [40], suggesting that *B. pertussis* could produce an extracellular *N*-acetyl galactosaminuronic acid Vi antigen-like polymer. Interestingly, this is an acidic-type polysaccharide, which is consistent with FT-IR data and the light microscopy examination showing alcian blue-stained material associated with biofilm cells (Fig. 7). It is worthy to note that other proteins encoded in both loci mostly correspond to putative glycosyltransferase enzymes with p*I* values predicted to be between 9.4 and 11.1, which was out of the range of the proteome analysis performed within this work. Finally, the third protein, which was only detected in the biofilm, is termed thymidine diphosphoglucose 4,6-dehydratase (BP0665). It corresponds to a nucleoside epimerase/dehydratase suggested to be involved in cell envelope biogenesis. Although encoded in different genomic regions, the activity of these enzymes seems to be closely related.

Several studies including a variety of bacteria provided evidence for a link between biofilm development and polysaccharide biosynthesis reviewed in ref. [41, 42], nevertheless no capsular or slime polysaccharides have been isolated or characterized for *Bordetella* yet. Recently, Parise *et al.* [22] reported the expression of a polysaccharide (Bps) biochemically similar to poly-β-1,6-*N*-acetyl-D-glucosamine polymer during the biofilm lifestyle of some *Bordetella* species, and Sloan *et al.* [3] showed that Bps is critical for biofilm formation of *B. bronchiseptica* in the respiratory tract of a mouse model. The results presented here from proteome and FT-IR analysis suggest the expression of an acidic-type polysaccharide by *B. pertussis*, probably an *N*-acetyl galactosaminuronic acid-like polymer (see Table 1 and Fig. 7). These studies consistently show that biofilm formation markedly induces the biosynthesis of carbohydrate polymers in *Bordetella*. However, our finding of an acidic-type polysaccharide instead of a poly-β-1,6-*N*-acetyl-D-glucosamine polymer, one of the most common exopolysaccharide compound in biofilms [43], could also be a hint that the polysaccharide composition of *Bordetella* biofilms is rather complex, including several different extracellular polysaccharides. Further studies will be needed to clarify if (i) the different exopolysaccharides are produced simultaneously or sequentially, if (ii) the composition of exopolysaccharides varies between the different *Bordetella* species and (iii)

what specific properties do the different exopolysaccharides provide the bacteria. So far, evidence is lacking that polysaccharides are important for growth or survival of *Bordetella* in alternative conditions other than biofilms. The production of a polysaccharide matrix might therefore represent a key factor for the survival of *B. pertussis* as a biofilm, contributing to the ability of the bacterium to withstand host defence mechanisms.

Furthermore, significant changes in abundance of virulence related proteins were noted (see Table 1). For example the autotransporter pertactin, other putative adhesins such as BipA and the prominent outer membrane porin protein BP0840 [44–46] were significantly upregulated in biofilm. For a number of microorganisms the expression of surface proteins, like BapA in *Staphylococcus aureus* and Ag43 in *Escherichia coli* [47, 48], has been reported to be essential for proper biofilm formation. It is tempting to speculate that the adhesion factors shown to be over-expressed or expressed *de novo* in *B. pertussis* biofilms might play a similar role in maturation of *B. pertussis* biofilms. However, this process seems to be rather complex involving various factors. For example biofilm formation is significantly reduced but not abolished in a knock out mutant of the Bvg regulated virulence factor pertactin (see Fig. S4 of Supporting Information). It is well known that inactivation of single genes might not necessarily results in an altered phenotype since the effected gene products might be compensated by other proteins of similar functions [49].

In addition, changes were observed in the spot pattern of the BvgA transcriptional activator, which indicate changes in its phosphorylation status (see Fig. 2B). In *Bordetella*, BvgA, together with the sensor protein BvgS, integrates the BvgAS two-component system, which controls the expression of a complex array of virulence factors through a phosphorylation cascade in response to environmental stimuli [50]. The recent finding that the BvgAS system is involved in regulating biofilm formation [2, 4, 20] together with the results presented in this work, raise intriguing questions about the virulence phenotype of the sessile cells. Another interesting observation, which requires further attention, is the increased expression of S-adenosylmethionine synthetase in biofilm. This enzyme plays an important role in quorum sensing, a regulatory process intimately related to biofilm [51, 52], but not yet described for *Bordetella*.

In conclusion, the distinctiveness of the *B. pertussis* biofilm physiology could be demonstrated by coupling, for the first time, proteomic and FT-IR spectroscopy tools with multivariate statistical methods. The production of a putative acidic-type polysaccharide polymer turned out to be the most distinctive feature of sessile physiology, and it is tempting to speculate that this polysaccharide might play an important role in *B. pertussis* pathogenesis and longtime persistence in the host. Most of the physiological studies in *B. pertussis*, and even the therapeutic strategies to control the disease, have traditionally been based on the use of planktonic cultures [53, 54]. However, this work using 2-DE and FT-IR as complementary techniques highlights the importance of biofilm-related studies to gain insight into the mechanisms underlying longtime persistence of *B. pertussis* within the host. Our work forms the starting point for a more detailed analysis to decipher the link between virulence and biofilm formation, and it may also help find new targets against human infections.

D. O. S. has a doctoral fellowship from CONICET. D. O. S is grateful to the DAAD (German Academic Exchange Service, Bonn, Germany) for a fellowship award. We kindly thank Monica Dommel for proof reading of the manuscript.

The authors have declared no conflict of interest.

5 References

[1] Cherry, J. D., The epidemiology of pertussis: A comparison of the epidemiology of the disease pertussis with the epidemiology of *Bordetella pertussis* infection. *Pediatrics* 2005, *115*, 1422–1427.

[2] Serra, D., Bosch, A., Russo, D. M., Rodriguez, M. E. *et al.*, Continuous nondestructive monitoring of *Bordetella pertussis* biofilms by Fourier transform infrared spectroscopy and other corroborative techniques. *Anal. Bioanal. Chem.* 2007, *387*, 1759–1767.

[3] Sloan, G. P., Love, C. F., Sukumar, N., Mishra, M., Deora, R., The *Bordetella* Bps polysaccharide is critical for biofilm development in the mouse respiratory tract. *J. Bacteriol.* 2007, *189*, 8270–8276.

[4] Irie, Y., Mattoo, S., Yuk, M. H., The Bvg virulence control system regulates biofilm formation in *Bordetella bronchiseptica*. *J. Bacteriol.* 2004, *186*, 5692–5698.

[5] Costerton, J. W., Stewart, P. S., Greenberg, E. P., Bacterial biofilms: A common cause of persistent infections. *Science* 1999, *284*, 1318–1322.

[6] Hall-Stoodley, L., Costerton, J. W., Stoodley, P., Bacterial biofilms: From the natural environment to infectious diseases. *Nat. Rev. Microbiol.* 2004, *2*, 95–108.

[7] Mattoo, S., Cherry, J. D., Molecular pathogenesis, epidemiology, and clinical manifestations of respiratory infections due to *Bordetella pertussis* and other *Bordetella subspecies*. *Clin. Microbiol. Rev.* 2005, *18*, 326–382.

[8] Donlan, R. M., Costerton, J. W., Biofilms: Survival mechanisms of clinically relevant microorganisms. *Clin. Microbiol. Rev.* 2002, *15*, 167–193.

[9] Beloin, C., Valle, J., Latour-Lambert, P., Faure, P. *et al.*, Global impact of mature biofilm lifestyle on *Escherichia coli* K-12 gene expression. *Mol. Microbiol.* 2004, *51*, 659–674.

[10] Waite, R. D., Papakonstantinopoulou, A., Littler, E., Curtis, M. A., Transcriptome analysis of *Pseudomonas aeruginosa* growth: Comparison of gene expression in planktonic cultures and developing and mature biofilms. *J. Bacteriol.* 2005, *187*, 6571–6576.

[11] Spoering, A. L., Lewis, K., Biofilms and planktonic cells of *Pseudomonas aeruginosa* have similar resistance to killing by antimicrobials. *J. Bacteriol.* 2001, *183*, 6746–6751.

[12] Ghigo, J. M., Are there biofilm-specific physiological pathways beyond a reasonable doubt? *Res. Microbiol.* 2003, *154*, 1–8.

[13] Nandakumar, R., Nandakumar, M. P., Marten, M. R., Ross, J. M., Proteome analysis of membrane and cell wall associated proteins from *Staphylococcus aureus*. *J. Proteome Res.* 2005, *4*, 250–257.

[14] Tremoulet, F., Duche, O., Namane, A., Martinie, B., Labadie, J. C., A proteomic study of *Escherichia coli* O157:H7 NCTC 12900 cultivated in biofilm or in planktonic growth mode. *FEMS Microbiol. Lett.* 2002, *215*, 7–14.

[15] Marengo, E., Robotti, E., Bobba, M., Multivariate statistical tools for the evaluation of proteomic 2D-maps: Recent achievements and applications. *Curr. Proteomics* 2007, *4*, 53–66.

[16] Vilain, S., Cosette, P., Hubert, M., Lange, C. *et al.*, Comparative proteomic analysis of planktonic and immobilized *Pseudomonas aeruginosa* cells: A multivariate statistical approach. *Anal. Biochem.* 2004, *329*, 120–130.

[17] Vilain, S., Brozel, V. S., Multivariate approach to comparing whole-cell proteomes of *Bacillus cereus* indicates a biofilm-specific proteome. *J. Proteome Res.* 2006, *5*, 1924–1930.

[18] Naumann, D., Helm, D., Labischinski, H., Microbiological characterizations by FT-IR spectroscopy. *Nature* 1991, *351*, 81–82.

[19] Nichols, P. D., Henson, J. M., Guckert, J. B., Nivens, D. E., White, D. C., Fourier transform-infrared spectroscopic methods for microbial ecology: Analysis of bacteria, bacteria-polymer mixtures and biofilms. *J. Microbiol. Methods* 1985, *4*, 79–94.

[20] Mishra, M., Parise, G., Jackson, K. D., Wozniak, D. J., Deora, R., The BvgAS signal transduction system regulates biofilm development in *Bordetella*. *J. Bacteriol.* 2005, *187*, 1474–1484.

[21] Bosch, A., Serra, D., Prieto, C., Schmitt, J. *et al.*, Characterization of *Bordetella pertussis* growing as biofilm by chemical analysis and FT-IR spectroscopy. *Appl. Microbiol. Biotechnol.* 2006, *71*, 736–747.

[22] Parise, G., Mishra, M., Itoh, Y., Romeo, T., Deora, R., Role of a putative polysaccharide locus in *Bordetella* biofilm development. *J. Bacteriol.* 2007, *189*, 750–760.

[23] Naumann, D., Infrared spectroscopy in microbiology. In *Encyclopedia of Analytical Chemistry*, Wiley, Chichester 2000, pp. 102–131.

[24] Ehling-Schulz, M., Schulz, S., Wait, R., Görg, A., Scherer, S., The UV-B stimulon of the terrestrial cyanobacterium Nostoc commune comprises early shock proteins and late acclimation proteins. *Mol. Microbiol.* 2002, *46*, 827–843.

[25] Turlin, E., Pascal, G., Rousselle, J. C., Lenormand, P. *et al.*, Proteome analysis of the phenotypic variation process in *Photorhabdus luminescens*. *Proteomics* 2006, *6*, 2705–2725.

[26] Görg, A., Obermaier, C., Boguth, G., Harder, A. *et al.*, The current state of two-dimensional electrophoresis with immobilized pH gradients. *Electrophoresis* 2000, *21*, 1037–1053.

[27] Görg, A., Weiss, W., Dunn, M. J., Current two-dimensional electrophoresis technology for proteomics. *Proteomics* 2004, *4*, 3665–3685.

[28] Manly, B. F. J., *Multivariate Statistical Methods: A Primer*, 2nd Edn, Chapman & Hall, London 1994.

[29] Kacuráková, M., Capek, P., Sasinkova, V., Wellner, N., Ebringerová, A., FT-IR study of plant cell wall model compounds: Pectic polysaccharides and hemicelluloses. *Carbohydr. Polym.* 2000, *43*, 195–203.

[30] Nivens, D. E., Ohman, D. E., Williams, J., Franklin, M. J., Role of alginate and its O acetylation in formation of *Pseudomonas aeruginosa* microcolonies and biofilms. *J. Bacteriol.* 2001, *183*, 1047–1057.

[31] Synytsya, A., Copikova, J., Matejka, P., Machovic, V., Fourier transform Raman and infrared spectroscopy of pectins. *Carbohydr. Polym.* 2003, *54*, 97–106.

[32] Moreno, J., Vargas, M. A., Madiedo, J. M., Munoz, J. *et al.*, Chemical and rheological properties of an extracellular polysaccharide produced by the cyanobacterium *Anabaena* sp. ATCC 33047. *Biotechnol. Bioeng.* 2000, *67*, 283–290.

[33] Tremoulet, F., Duche, O., Namane, A., Martinie, B., Labadie, J. C., Comparison of protein patterns of *Listeria monocytogenes* grown in biofilm or in planktonic mode by proteomic analysis. *FEMS Microbiol. Lett.* 2002, *210*, 25–31.

[34] Resch, A., Leicht, S., Saric, M., Pasztor, L. *et al.*, Comparative proteome analysis of *Staphylococcus aureus* biofilm and planktonic cells and correlation with transcriptome profiling. *Proteomics* 2006, *6*, 1867–1877.

[35] Mikkelsen, H., Duck, Z., Lilley, K. S., Welch, M., Interrelationships between colonies, biofilms, and planktonic cells of *Pseudomonas aeruginosa*. *J. Bacteriol.* 2007, *189*, 2411–2416.

[36] Whiteley, M., Bangera, M. G., Bumgarner, R. E., Parsek, M. R. *et al.*, Gene expression in *Pseudomonas aeruginosa* biofilms. *Nature* 2001, *413*, 860–864.

[37] Hancock, R. E., A brief on bacterial biofilms. *Nat. Genet.* 2001, *29*, 360.

[38] Jouenne, T., Vilain, S., Cosette, P., Junter, G. A., Proteomics of biofilm bacteria. *Curr. Proteomics* 2004, *1*, 211–219.

[39] Parkhill, J., Sebaihia, M., Preston, A., Murphy, L. D. *et al.*, Comparative analysis of the genome sequences of *Bordetella pertussis*, *Bordetella parapertussis* and *Bordetella bronchiseptica*. *Nat. Genet.* 2003, *35*, 32–40.

[40] Virlogeux, I., Waxin, H., Ecobichon, C., Popoff, M. Y., Role of the viaB locus in synthesis, transport and expression of *Salmonella typhi* Vi antigen. *Microbiology* 1995, *141*, 3039–3047.

[41] Branda, S. S., Vik, S., Friedman, L., Kolter, R., Biofilms: The matrix revisited. *Trends Microbiol.* 2005, *13*, 20–26.

[42] Sutherland, I., Biofilm exopolysaccharides: A strong and sticky framework. *Microbiology* 2001, *147*, 3–9.

[43] Lasa, I., Towards the identification of the common features of bacterial biofilm development. *Int. Microbiol.* 2006, *9*, 21–28.

[44] Emsley, P., Charles, I. G., Fairweather, N. F., Isaacs, N. W., Structure of *Bordetella pertussis* virulence factor P.69 pertactin. *Nature* 1996, *381*, 90–92.

[45] Stockbauer, K. E., Fuchslocher, B., Miller, J. F., Cotter, P. A., Identification and characterization of BipA, a *Bordetella* Bvg-intermediate phase protein. *Mol. Microbiol.* 2001, *39*, 65–78.

[46] Li, Z. M., Hannah, J. H., Stibitz, S., Nguyen, N. Y. *et al.*, Cloning and sequencing of the structural gene for the porin protein of *Bordetella pertussis*. *Mol. Microbiol.* 1991, *5*, 1649–1656.

[47] Cucarella, C., Solano, C., Valle, J., Amorena, B. *et al.*, Bap, a *Staphylococcus aureus* surface protein involved in biofilm formation. *J. Bacteriol.* 2001, *183*, 2888–2896.

[48] Van Houdt, R., Michiels, C. W., Role of bacterial cell surface structures in *Escherichia coli* biofilm formation. *Res. Microbiol.* 2005, *156*, 626–633.

[49] Jakob, K., Satorhelyi, P., Lange, C., Wendisch, V. F. *et al.*, Gene expression analysis of *Corynebacterium glutamicum* subjected to long-term lactic acid adaptation. *J. Bacteriol.* 2007, *89*, 5582–5590.

[50] Cotter, P. A., Jones, A. M., Phosphorelay control of virulence gene expression in *Bordetella*. *Trends Microbiol.* 2003, *11*, 367–373.

[51] Schauder, S., Shokat, K., Surette, M. G., Bassler, B. L., The LuxS family of bacterial autoinducers: Biosynthesis of a novel quorum-sensing signal molecule. *Mol. Microbiol.* 2001, *41*, 463–476.

[52] Miller, M. B., Bassler, B. L., Quorum sensing in bacteria. *Annu. Rev. Microbiol.* 2001, *55*, 165–199.

[53] Graeff-Wohlleben, H., Deppisch, H., Gross, R., Global regulatory mechanisms affect virulence gene expression in *Bordetella pertussis*. *Mol. Gen. Genet.* 1995, *247*, 86–94.

[54] Martinez de Tejada, G., Miller, J. F., Cotter, P. A., Comparative analysis of the virulence control systems of *Bordetella pertussis* and *Bordetella bronchiseptica*. *Mol. Microbiol.* 1996, *22*, 895–908.

